HYDROELASTIC RESPONSE OF SLENDER COMPOSITE HULLS SUBJECTED TO SLAMMING IMPACT

Liviu Librescu*, Zhanming Qin [Zhanming Qin]: e-mail zqin@vt.edu**
Virginia Tech, Blacksburg, VA 24061-0219, USA

*Professor, Department of Engineering Science and Mechanics. Deceased on Apr.16, 2007.
** Research Scientist, Department of Engineering Science and Mechanics

Keywords: *hydroelastic response, slamming impact, composite hulls, elastic tailoring*

Abstract

In the context of marine vehicles made of advanced composite materials and of related structural components, the present work is devoted to the development of a dynamic hydroelastic response model. Toward this end, a moderately thick-walled anisotropic beam theory is used to idealize the load-carrying structural part of the hulls. The multitude of exotic elastic couplings provided by anisotropy and lay-ups are incorporated. By integrating the unsteady hydrodynamic loading mode, the governing hydroelastic equations in a special case of circumferentially asymmetric stiffness (CAS) lay-up are developed. The concept of elastic tailoring is exploited for the alleviation of the dynamic response of the hulls subject to slamming impact. It is demonstrated that the directionality property of composite materials and lamination lay-ups are efficient on the reduction of whipping response.

1 Introduction

To facilitate the design of marine vehicles, various structural and hydroelastic models based on beam theories have been developed to predict, in the preliminary design stage, their dynamic behavior and stability, see e.g., [1-7]. However, in the context of marine vehicles made of *composite materials*, there is a total absence of such studies. Compared with the Euler-Bernoulli, Timoshenko and Vlasov's metallic beam-like structural models (see e.g., [8]), their composite counterparts, due to their inherent material directionality and lamination lay-ups, can bring a dramatic enhancement of their performance. Such enhancement can be attained by the *elastic* and *hydroelastic tailoring*. The former approach consists in the proper use and exploitation of the anisotropy of the involved materials and lay-up lamination to effectively modify the distribution of the structural stiffness, while the latter one is to modify, by exploiting the anisotropy of the materials and lay-up lamination, the hydroelastic coupling such that the structural response and/or stability can be enhanced. The objective of the first approach is to change the stiffness distribution while the second approach benefits mainly from the enhanced fluid-structure interaction. In the context of aeronautical structures, the counterpart techniques referred to as the *aeroelastic tailoring* has been successfully used to address the chronic divergence problem of forward-swept wings, as demonstrated by Grumman X-29 aircraft [8].

As a prerequisite toward implementation of elastic and hydroelastic tailoring, a number of issues have to be investigated, which include:

- Multitude of elastic couplings, which involves various couplings among bending, twist, extension, transverse shearing, etc.;
- Implication of non-classical effects such as of transverse shear and of warping (restraint) in the context of anisotropy of the materials and the moderate thickness of the hull's walls.

In this paper, a refined first-order transverse shearable anisotropic beam theory, which was originally developed and validated in a number of previous works by [9-12] will be used to model the moderately thick-walled composite hulls. By integrating the unsteady hydrodynamic loads, the governing hydroelastic equations will be fully derived for the special lay-up case of circumferentially asymmetric stiffness (CAS) configuration. As will be shown in the sequel, this CAS configuration can provide two sets of independent elastic couplings: (1)vertical bending/vertical transverse shear/extension; and (2)horizontal bending/horizontal transverse shear/twist. These two sets idealize the couplings of motions encountered in practice (see e.g., [4, 6]).

Although an actual hull is of considerable complexity in its shape, here we restrict ourselves to the case of the uniform, closed cross-section beams.

The derived governing equations are then applied toward the investigation of the hydroelastic response of the hulls subject to bottom slamming-like impact. It is well known that the impact can cause both severe local damage on the composite/sandwich hulls [13], and simultaneously, global high-frequency vibrations that accelerate their fatigue failure. However, as pointed out by [14], when the duration of the bottom slamming-type impact is much smaller than the low-range global natural periods, the global and local effects of the impact can be investigated separately. In the present paper, we will focus only on the global slamming response of composite hull due to bottom slamming-type impact and investigate the effectiveness of the tailoring on its alleviation.

2 Coordinate Systems

The load-carrying part of the hull is idealized as a composite moderately thick-walled beam (see Figs.1 and 2) and the hull is assumed to symmetric with respect to z-axis.

Two set of body-fixed right-hand Cartesian coordinate systems are adopted here with positive x direction to be along the mean forward speed $\bar{U}$ of the ship:

- (x, y, z) : consisting of the three intersection lines of the three geometric symmetric planes. The origin o_{xyz} is at the intersection of the after perpendicular and x-axis and located at the depth H_w from the free water surface. This coordinate system is used in the structural modeling;
- (ξ, η, ς) : the plane $\varsigma = 0$ corresponds to the calm water level, and ς is positive upwards. The origin $o_{\xi\eta\varsigma}$ is at the intersection of the after perpendicular and ς-axis. This coordinate system is used in the formulation of hydrodynamic loading. In the sequel, the cross section of the wetted hull surface is denoted by $\bar{S}(\xi)$ or $\bar{S}(x)$, and the coordinates $\eta = \eta(\ell)$, $\varsigma = \varsigma(\ell)$, where ℓ is a parameter to identify the location of a point on $\bar{S}(\xi)$.

3 Structural Modeling

3.1 Kinematics of a Moderately Thick-Walled Composite Hull by the First-Order Theory

The displacement field of the hull can be postulated as

$$u_1(x,y,z,t) = u_{10}(x,t) + \left[z_s(s) - n\frac{dy_s(s)}{ds} \right]\theta_y(x,t) - \left[y_s(s) + n\frac{dz_s(s)}{ds} \right]\theta_z(x,t) - \left[F_w(s) + na(s)\right]\phi'(x,t) \tag{1a}$$

$$u_2(x,y,z,t) = u_{20}(x,t) - z\phi(x,t) \tag{1b}$$

$$u_3(x,y,z,t) = u_{30}(x,t) + y\phi(x,t) \tag{1c}$$

where, the prime $()' \equiv \partial()/\partial x$, and $\theta_y = \gamma_{xz} - u'_{30}$ denotes the rotation of the cross section with respect to axis y , while $\theta_z = u'_{20} - \gamma_{xy}$ denotes the rotation of the cross section with respect to axis z; y_s and z_s correspond to the coordinates of point (*x*,*y*,*z*) in the local coordinate system by prescribing $n = 0$ (i.e., on the mid-contour), and $a(s) \equiv -z_s\frac{dz_s}{ds} - y_s\frac{dy_s}{ds}$; u_{10} , u_{20} and u_{30} are measures of the overall displacements of the cross section in x , y and z axes, respectively; ϕ denotes the rotations of the cross section about x axes, respectively. The warping function of the cross section F_w is defined as:

$$F_w(s) = \int_0^s \left[r_n(\tau) - \aleph(\tau)\right]d\tau \tag{2}$$

in which, $\aleph$ is the torsional function of the hull's cross section and the quantity

$$r_n(s) \equiv y_s\frac{dz_s}{ds} - z_s\frac{dy_s}{ds} \tag{3}$$

Within the frame of first-order beam theory, one obtains:

$$y = y_s + n\frac{dz_s}{ds}, \; z = z_s - n\frac{dy_s}{ds} \tag{4}$$

3.2 Internal Forces in the Hull

Define the following membrane and transverse shear stress resultants

$$\begin{Bmatrix} N_{ss} \\ N_{xx} \\ N_{sx} \\ N_{xn} \\ N_{sn} \end{Bmatrix} = \sum_k \int_{n^{(k-1)}}^{n^{(k)}} \begin{Bmatrix} \sigma_{ss} \\ \sigma_{xx} \\ \sigma_{sx} \\ \sigma_{xn} \\ \sigma_{sn} \end{Bmatrix} dn \tag{5}$$

and the following stress couples

$$\begin{Bmatrix} L_{xx} \\ L_{sx} \end{Bmatrix} = \sum_k \int_{n^{(k-1)}}^{n^{(k)}} \begin{Bmatrix} \sigma_{xx} \\ \sigma_{sx} \end{Bmatrix} ndn \tag{6}$$

By virtue of the assumption related to the transverse normal stress $\sigma_{nn} = 0$ and to the hoop stress resultant $N_{ss} = 0$ [15], the 2-D stress resultants and stress couples can be reduced to the following expressions:

$$\begin{bmatrix} N_{xx} \\ N_{sx} \\ L_{xx} \\ L_{sx} \end{bmatrix} = \begin{bmatrix} K_{11} & K_{12} & K_{13} & K_{14} \\ K_{21} & K_{22} & K_{23} & K_{24} \\ K_{41} & K_{42} & K_{43} & K_{44} \\ K_{51} & K_{52} & K_{53} & K_{54} \end{bmatrix} \begin{Bmatrix} \varepsilon_{xx}^{(0)} \\ \gamma_{sx}^{(0)} \\ \phi' \\ \varepsilon_{xx}^{(1)} \end{Bmatrix} \tag{7}$$

$$N_{nx} = [A_{44} - \frac{A_{45}^2}{A_{55}}]\gamma_{xn} \tag{8}$$

in which, K_{ij} are the reduced stiffness coefficients; $\varepsilon_{xx}^{(0)}$ and $\gamma_{xx}^{(0)}$ are the normal and shear strain components on the mid-surface of the beam walls, $\varepsilon_{xx}^{(1)}$ is the first-order normal strain, whereas γ_{xn} is the 2-D transverse shear strain. The expressions of these quantities are provided by

$$\varepsilon_{xx}^{(0)} = u_{10}' + z_s\theta_y' - y_s\theta_z' - F_w\phi'' \tag{9a}$$

$$\gamma_{sx}^{(0)} = \frac{dy_s}{ds}(u_{20}' - \theta_z) + \frac{dz_s}{ds}(u_{30}' + \theta_y)\aleph(s)\phi' \tag{9b}$$

$$\varepsilon_{sx}^{(1)} = -\frac{dy_s}{ds}\theta_y' - \frac{dz_s}{ds}\theta_z' - a_w\phi'' \tag{9c}$$

$$\gamma_{nx} = \frac{dz_s}{ds}(u_{20}' - \theta_z) - \frac{dy_s}{ds}(u_{30}' + \theta_y) \tag{9d}$$

We further define the following 1-D (beam) internal forces:

$$T_x(x,t) \equiv \oint N_{xx}(s)ds\,, \tag{10a}$$

$$Q_y \equiv \oint\left[N_{sx}\frac{dy_s}{ds} + N_{nx}\frac{dz_s}{ds}\right]ds\,, \tag{10b}$$

$$Q_z \equiv \oint\left[N_{sx}\frac{dz_s}{ds} - N_{nx}\frac{dy_s}{ds}\right]ds\,, \tag{10c}$$

$$M_y \equiv \oint\left[N_{xx}z_s - L_{xx}\frac{dy_s}{ds}\right]ds\,, \tag{10d}$$

$$M_z \equiv \oint\left[N_{xx}y_s - L_{xx}\frac{dz_s}{ds}\right]ds\,, \tag{10e}$$

$$B_w \equiv \oint\left[-N_{xx}F_w - L_{xx}a\right]ds\,, \tag{10f}$$

$$M_x \equiv \oint\left[N_{sx}\psi(s) + 2L_{sx}\right]ds \tag{10g}$$

in which and in the sequel, the closed-contour integration is carried out along the closed mid-line contour of the walls.

The internal force-displacement relation can be represented as

$$\begin{Bmatrix} T_x \\ M_y \\ M_z \\ Q_z \\ Q_y \\ B_w \\ M_x \end{Bmatrix} = \begin{bmatrix} a_{11} & a_{12} & a_{13} & a_{14} & a_{15} & a_{16} & a_{17} \\ a_{12} & a_{22} & a_{23} & a_{24} & a_{25} & a_{26} & a_{27} \\ a_{13} & a_{23} & a_{33} & a_{34} & a_{35} & a_{36} & a_{37} \\ a_{14} & a_{24} & a_{34} & a_{44} & a_{45} & a_{46} & a_{47} \\ a_{15} & a_{25} & a_{35} & a_{45} & a_{55} & a_{56} & a_{57} \\ a_{16} & a_{26} & a_{36} & a_{46} & a_{56} & a_{66} & a_{67} \\ a_{17} & a_{27} & a_{37} & a_{47} & a_{57} & a_{67} & a_{77} \end{bmatrix} \times \begin{Bmatrix} u_{10}' \\ \theta_y' \\ \theta_z' \\ u_{30}' + \theta_y \\ u_{20}' - \theta_z \\ \phi'' \\ \phi' \end{Bmatrix} \tag{11}$$

It is noted that the stiffness matrix in Eq.11 is symmetric, i.e., $a_{ij} = a_{ji}$, and the equation constitutes the most general representation of the force-displacement relations of moderately thick-walled anisotropic beams. In general, for anisotropic and heterogeneous materials, the stiffness matrix is fully populated, among which, the off-diagonal entries are associated with the structural couplings involving bending, twist, extension, transverse shearing and warping. Assessment of these couplings on the motion of composite naval hulls and their proper exploitation should constitute an important task toward a rational design of these structures and toward the proper use of the exotic material characteristics.

However, in the present paper, we will focus on a special lay-up configuration, namely the circumferentially asymmetric stiffness (CAS) with respect to the horizontal axis y (see e.g., [16]). Similar to the cases investigated by [17, 18], this type of beams feature the following two independent sets of elastic couplings:

- Vertical bending/vertical transverse shear/ extension (u_{30}, θ_y, u_{10});
- Horizontal bending/horizontal transverse shear/twist (u_{20}, θ_z, ϕ).

In such a case, the internal force-displacement relations split into two groups:

$$\begin{Bmatrix} M_z \\ Q_y \\ B_w \\ M_x \end{Bmatrix} = \begin{bmatrix} a_{33} & a_{35} & a_{36} & a_{37} \\ a_{35} & a_{55} & a_{56} & a_{37} \\ a_{36} & a_{56} & a_{66} & a_{67} \\ a_{37} & a_{57} & a_{67} & a_{77} \end{bmatrix} \begin{Bmatrix} \theta_z' \\ u_{20}' - \theta_z \\ \phi'' \\ \phi' \end{Bmatrix} \quad (12a)$$

$$\begin{Bmatrix} T_x \\ M_y \\ Q_z \end{Bmatrix} = \begin{bmatrix} a_{11} & a & a \\ a & a & a \\ a & a & a \end{bmatrix} \begin{Bmatrix} u_{10}' \\ \theta_y' \\ u_{30}' + \theta_y \end{Bmatrix} \quad (12b)$$

When the transverse shears are disregarded (referred to as the non-transverse shearable (NTS) model herein and in the sequel), $\theta_z \to u_{20}'$, and $\theta_y \to -u_{30}'$. Consequently, the counterparts of Eqs. 12a and 12b become:

$$\begin{Bmatrix} M_z \\ Q_y \\ B_w \\ M_x \end{Bmatrix} = \begin{bmatrix} a_{33} & a_{36} & a_{37} \\ a_{35} & a_{56} & a_{57} \\ a_{36} & a_{66} & a_{67} \\ a_{37} & a_{67} & a_{77} \end{bmatrix} \begin{Bmatrix} u_{20}'' \\ \phi'' \\ \phi' \end{Bmatrix} \quad (13a)$$

$$\begin{Bmatrix} T_x \\ M_y \\ Q_z \end{Bmatrix} = \begin{bmatrix} a_{11} & a_{12} \\ a_{12} & a_{22} \\ a_{14} & a_{24} \end{bmatrix} \begin{Bmatrix} u_{10}' \\ -u_{30}'' \end{Bmatrix} \quad (13b)$$

4 Governing Equations in the Case of CAS Lay-Up

The governing equations and the consistent boundary conditions can be systematically derived by using the extended Hamilton's principle [19]:

$$\int_{t_1}^{t_2} (\delta T - \delta U + \overline{\delta W}) dt = 0$$

with

$\delta u_0 = \delta v_0 = \delta w_0 = \delta\theta_y = \delta\theta_z = \delta\phi = 0$ at $t = t_1 \,\&\, t_2$

where δT and δU denote the virtual kinetic and strain energy, respectively, while $\overline{\delta W}$ denotes the virtual work due to external forces. For the problem at hand, these terms are defined as follows:

$$\delta T = \int_0^L \oint \sum_k \int_{n^{(k)}}^{n^{(k+1)}} \rho_s^{(k)} [\left(\frac{\partial u_1}{\partial t}\right) \delta\left(\frac{\partial u_1}{\partial t}\right) + \left(\frac{\partial u_2}{\partial t}\right) \delta\left(\frac{\partial u_2}{\partial t}\right) + \left(\frac{\partial u_3}{\partial t}\right) \delta\left(\frac{\partial u_3}{\partial t}\right)] dndsdx \quad (14a)$$

$$\delta U = \int_\tau \sigma_{ij} \delta\varepsilon_{ij} d\tau = \int_0^L \oint \sum_k \int_{n^{(k)}}^{n^{(k+1)}} [\sigma_{xx}\delta\varepsilon_{xx} + \sigma_{sx}\delta\gamma_{sx} + \sigma_{nx}\delta\gamma_{nx}] dndsdx \quad (14b)$$

$$\overline{\delta W} = \int_0^L [F_x(x,t)\delta u_{10}(x,t) + F_y(x,t)\delta u_{20}(x,t) + m_x(x,t)\delta\phi(x,t)] dx \quad (14c)$$

where, u_j ($j = 1-3$) are defined by Eqs. 1a-1c, whereas F_x, F_y and F_z are the hydrodynamic loads per unit span while m_x is the hydrodynamic twist moment per unit span about axis x. It is noted that in the present paper, only unsteady part of the hydrodynamic loads are considered.

The governing equations of the first group, which we will focus in the sequel, are

$$\delta u_{10}:\quad a_{11}u_{10}'' + a_{12}\theta_y'' + a_{14}(u_{30}'' + \theta_y') + F_x - b_1\ddot{u}_{10} = 0$$
$$\delta u_{30}:\quad a_{14}u_{10}'' + a_{24}\theta_y'' + a_{44}(u_{30}'' + \theta_y') + F_z - b_1\ddot{u}_{30} = 0$$
$$\delta\theta_y:\quad a_{12}u_{10}'' + a_{22}\theta_y'' + a_{24}(u_{30}'' + \theta_y') - a_{14}u_{10}' - a_{24}\theta_y' - a_{44}(u_{30}' + \theta_y) - b_6\ddot{\theta}_y = 0 \qquad \text{(15a-c)}$$

in which, b_1 and b_6 are the inertia coefficients.

The associated free-free boundary conditions expressed in terms of the displacement quantities can be summarized as:

At $x = 0$ or L

$$\delta u_{10}:\quad a_{11}u_{10}' + a_{12}\theta_y' + a_{14}(u_{30}' + \theta_y) = T_x(t)$$
$$\delta u_{30}:\quad a_{14}u_{10}' + a_{24}\theta_y' + a_{44}(u_{30}' + \theta_y) = 0$$
$$\delta\theta_y:\quad a_{12}u_{10}' + a_{22}\theta_y' + a_{24}(u_{30}' + \theta_y) = 0 \qquad \text{(16a-c)}$$

In the NTS model, the corresponding governing equations reduce to

$$\delta u_{10}:\quad a_{11}u_{10}'' - a_{12}u_{30}''' - b_1\ddot{u}_{10} = 0 \qquad \text{(17a,b)}$$
$$\delta u_{30}:\quad a_{14}u_{10}'' - a_{22}u_{30}^{(IV)} + F_z - b_1\ddot{u}_{30} + b_6 u_{30}'' = 0$$

and the associated free-free boundary conditions become:

At $x = 0$ or L

$$\delta u_{10}:\quad a_{11}u_{10}' - a_{12}u_{30}'' = T_x(t)$$
$$\delta u_{30}:\quad a_{12}u_{10}'' - a_{22}u_{30}''' - b_6\ddot{u}_{30}' = 0$$
$$\delta u_{30}':\quad a_{12}u_{10}' - a_{22}u_{30}'' = 0 \qquad \text{(18a-c)}$$

In the normal operational conditions, due to the much higher ratio of force over hull stiffness in the longitudinal direction as compared to the vertical and lateral ones, the deformation of the hull in the longitudinal direction u_{10} can be completely disregarded. As a result, the governing equations reduce to

$$\delta u_{30}:\quad a_{24}\theta_y'' + a_{44}(u_{30}'' + \theta_y') + F_z - b_1\ddot{u}_{30} = 0 \qquad \text{(19a,b)}$$
$$\delta\theta_y:\quad a_{22}\theta_y'' + a_{24}u_{30}'' - a_{44}(u_{30}' + \theta_y) - b_6\ddot{\theta}_y = 0$$

The associated free-free boundary conditions are: at $x = 0$ or L

$$\delta u_{30}:\quad a_{24}\theta_y' + a_{44}(u_{30}' + \theta_y) = 0 \qquad \text{(20a)}$$
$$\delta\theta_y:\quad a_{22}\theta_y' + a_{24}(u_{30}' + \theta_y) = 0 \qquad \text{(20b)}$$

5 Unsteady Hydroelastic Loads Acting on the Hull

We consider the case that the wetted surface of the hull is symmetric about the z-axis. Details of the derivation are omitted here. The final expression of the unsteady hydroelastic load F_z can be summarized as:

$$F_z(x,t) = -\rho g u_{30}(x,t)\int_{\bar{S}(x)} d\eta - \rho\int_{\bar{S}(x)} \frac{\partial(\varphi_D + \varphi_I)}{\partial t}d\eta - \overline{m}_{22}(x)\ddot{u}_{30}(x,t) - \int_0^t \dot{u}_{30}(x,t_2)h_{22}(x,t-t_2)dt_2 \qquad \text{(21)}$$

in which, ρ is mass density of the water, g is the acceleration of the gravity, $\overline{m}_{22}$ is the added mass of the hull's cross section when the oscillating frequency goes to infinity, φ_D and φ_I are the velocity potential associated with diffraction and incident waves, respectively; whereas h_{22} denotes the unsteady hydrodynamic impulsive function, which can be obtained either via experiments or numerical calculation.

6 Solution Approach

Due to the nonconservative nature of the problem and the complexities arising from the anisotropy of the constituent materials and the free-free boundary conditions, spatial semi-discretization techniques is adopted and the governing equations are cast into state-space form. The spatial semi-discretization is based on the modal analysis of the corresponding dry hull, while the conversion of the governing equations into state-space form is prompted by the fact that for a general nonconservative system, the solution requires a state-space description ([19], pp 206-210). Moreover, such a representation can be conveniently used in the case of the incorporation of an active control capability. In the sequel, we will present the description of the modal analysis, while the state-space approximation will be presented elsewhere.

Define the dimensionless longitudinal coordinate $\hat{x} \equiv x/L$. For the analysis of free vibration of the dry hull, one assumes the solution in the form:

$$u_{30}(\hat{x},t) = \overline{u}_{30}(\hat{x})\exp(i\omega t) \qquad \text{(22a)}$$
$$\theta_y(\hat{x},t) = \theta_y(\hat{x})\exp(i\omega t) \qquad \text{(22b)}$$

in which, $i \equiv \sqrt{-1}$, while ω denotes the vibration frequency.

Substituting these expressions in Eqs. 22a, b, the following ordinary differential equations are obtained:

$$\rho_s^2 \bar{\theta}_y'' - (1 - \rho_r^2 \rho_s^2 \rho_b^2)\bar{\theta}_y - \frac{1}{L}\bar{u}_{30}' = 0 \quad (23a)$$

$$\bar{u}_{30}'' + \rho_s^2 \rho_b^2 \bar{u}_{30} + L\bar{\theta}_y' = 0 \quad (23b)$$

in which, $\overline{(\bullet)'} \equiv \partial(\bullet)/\partial\hat{x}$, and the dimensionless parameters ρ_r, ρ_s and ρ_b are defined as:

$$\rho_s \equiv \sqrt{\frac{a_{22}}{a_{44}L^2}}, \rho_r \equiv \sqrt{\frac{b_6}{b_1 L^2}}, \rho_b \equiv \sqrt{\frac{b_1 L^4}{a_{22}}}\omega \quad (24a\text{-}c)$$

Following the approach by [20], after eliminating $\bar{u}_{30}(\hat{x})$ in Eq. 23a or $\bar{\theta}_y(\hat{x})$ in Eq. 23b, the governing equations for $\bar{u}_{30}(\hat{x})$ and $\bar{\theta}_y(\hat{x})$ are obtained as:

$$\bar{u}_{30}^{(IV)} + (\rho_s^2 + \rho_r^2)\rho_b^2 \bar{u}_{30}'' - (1 - \rho_s^2 \rho_r^2 \rho_b^2)\rho_b^2 \bar{u}_{30} = 0$$

$$\bar{\theta}_y^{(IV)} + (\rho_s^2 + \rho_r^2)\rho_b^2 \bar{\theta}_y'' - (1 - \rho_s^2 \rho_r^2 \rho_b^2)\rho_b^2 \bar{\theta}_y = 0$$

(25a,b)

It is noted that $\bar{u}_{30}(\hat{x})$ and $\bar{\theta}_y(\hat{x})$ fulfill the same governing equation. As a result, we only focus on the solution associated with $\bar{u}_{30}(\hat{x})$. Assume in Eq.24a the solution form $\bar{u}_{30}(\hat{x}) = \overline{\overline{u}}_{30} \exp(\lambda\hat{x})$, wherefrom one obtains

$$\lambda^2 = \frac{-\rho_b^2(\rho_s^2 + \rho_r^2) \pm \sqrt{(\rho_s^2 - \rho_r^2)^2 \rho_b^4 + 4\rho_b^2}}{2} \quad (26)$$

Within the practical low frequency range encountered by the global hydroelastic analysis, we have

$$\rho_b^2(\rho_s^2 + \rho_r^2) \le \sqrt{(\rho_s^2 - \rho_r^2)^2 \rho_b^4 + 4\rho_b^2} \quad (27)$$

As a result, two roots of λ in Eq. 26 should be nonnegative. Consequently, the four roots of λ can be written as

$$\lambda_{1,2} = \pm\left[-\frac{\rho_b^2(\rho_s^2 + \rho_r^2)}{2} + \sqrt{\left(\frac{\rho_s^2 - \rho_r^2}{2}\right)^2 \rho_b^2 + \rho_b^2}\right]^{1/2}$$

$$\lambda_{3,4} = \pm i\left[-\frac{\rho_b^2(\rho_s^2 + \rho_r^2)}{2} + \sqrt{\left(\frac{\rho_s^2 - \rho_r^2}{2}\right)^2 \rho_b^2 + \rho_b^2}\right]^{1/2}$$

(28a,b)

As a result, the solution form of $\bar{u}_{30}(\hat{x})$ can be represented as

$$\bar{u}_{30}(\hat{x}) = c_1\cosh(\lambda_1\hat{x}) + c_2\sinh(\lambda_1\hat{x}) + c_3\cos(\lambda_3\hat{x}) + c_4\sin(\lambda_3\hat{x}) \quad (29)$$

where, the parameters c_i ($i = 1-4$) need to be determined by the fulfillment of the boundary conditions. Substituting Eq. 29 into Eqs.23b, the solution of $\bar{\theta}_y(\hat{x})$ can be represented as:

$$\bar{\theta}_y(\hat{x}) = d_1\sinh(\lambda_1\hat{x}) + d_2\cosh(\lambda_1\hat{x}) + d_3\sin(\lambda_3\hat{x}) + d_4\sin(\lambda_3\hat{x}) \quad (30)$$

in which, the coefficients d_i ($i = 1-4$) are defined as

$$d_1 \equiv \left(-\frac{\lambda_1}{L} - \frac{\rho_s^2\rho_b^2}{L\lambda_1}\right)c_1,\ d_2 \equiv \left(-\frac{\lambda_1}{L} - \frac{\rho_s^2\rho_b^2}{L\lambda_1}\right)c_2$$

$$d_3 \equiv \left(\frac{\lambda_3}{L} - \frac{\rho_s^2\rho_b^2}{L\lambda_3}\right)c_3,\ d_4 \equiv \left(-\frac{\lambda_3}{L} + \frac{\rho_s^2\rho_b^2}{L\lambda_3}\right)c_4$$

(31a-d)

Fulfillment of the boundary conditions Eqs. 20a, b and the condition of nontriviality of the parameters c_i lead to the following transcendental characteristic equation:

$$2 - 2\cosh\lambda_1\cos\lambda_3 + \frac{\rho_b}{\sqrt{1 - \rho_b^2\rho_r^2\rho_s^2}} \times [\rho_b^2\rho_r^2 \times (\rho_r^2 - \rho_s^2)^2 + (3\rho_r^2 - \rho_s^2)]\sinh\lambda_1\sin\lambda_3 = 0 \quad (32)$$

The *n*th eigenmode corresponding to u_{30} and θ_y can be represented as

$$\bar{U}_{30}(n,\hat{x}) = c_{1n}\cosh(\lambda_{1n}\hat{x}) + c_{2n}\sinh(\lambda_{1n}\hat{x}) + c_3\cos(\lambda_{3n}\hat{x}) + c_4\sin(\lambda_{3n}\hat{x}) \quad (33a)$$

$$\bar{\Theta}_y(n,\hat{x}) = d_{1n}\sinh(\lambda_{1n}\hat{x}) + d_{2n}\cosh(\lambda_{1n}\hat{x}) + d_{3n}\sin(\lambda_{3n}\hat{x}) + d_{4n}\sin(\lambda_{3n}\hat{x}) \quad (33b)$$

By the expansion theorem [19], the general hydroelastic response in Eqs. 19a,b can be represented as

$$\hat{u}_{30}(\hat{x},t) = \sum_{n=1}^{\infty}\overline{U}_{30}(n,\hat{x})q_n(t) \tag{34a}$$

$$\hat{\theta}_y(\hat{x},t) = \sum_{n=1}^{\infty}\overline{\Theta}_y(n,\hat{x})q_n(t) \tag{34b}$$

In the practical implementation, the infinite series in the expressions Eqs. 34a,b will be truncated to a finite number.

7 Results and Discussion

Strictly speaking, bottom slamming impact is a nonlinear phenomenon, the amplitude and its time variation of the pressure are sensitive to the details of the impact, such as relative velocity between the hull and the ambient wave, wave slope, impact angle, local hull deadrise angle, etc.(see e.g., [21-24]). However, it is beyond our scope to deal with such details of the slamming impact. Instead, we restrict ourselves to the time-history of the slamming impact pressure in the case when its peak value and spatial distribution are given. More specifically, the following widely accepted empirical model (see e.g., [25, 26]) will be adopted:

$$F^{sl}(\hat{x},t) = F_{\max}(\hat{x})\left(\frac{t}{T_0}\right)\exp\left(1-\frac{t}{T_0}\right)$$

where, T_0 denotes the pressure rise time, while $F_{\max}(\hat{x})$ denotes the maximum slamming impact pressure per unit of $\hat{x}$.

In the following numerical calculation, it is assumed that the slamming impact uniformly acts on the 4th quarter of the hull, i.e., $\hat{x} \geq 0.75$. The material and geometrical properties of the hull are supplied in Table 1. In the following calculation, the ply angle on the webs is taken to be $\theta = 0$.

When a hull is subject to a slamming impact, high-frequency vibrations will be induced, which are referred to as whipping. It is well known that they can not be quenched easily either by the hydrodynamic damping (see e.g., [1]) or by the structural damping (see e.g., [26]). This is clearly demonstrated by Fig.3, in which the pressure rise time of the slamming impact is taken to be a typical one $T_0 = 0.033$ sec. (see e.g., [27]). Furthermore, it is assumed here that $L = 100m$, $F_{\max}(\hat{x}) = 10^6 N/m$, the added mass coefficient $\overline{m}_{22}$ and the added damping coefficient N_{22} are calculated on a wetted surface of the hull oscillating on the free surface.

During the past years, both passive and active mechanisms have been attempted for whipping reduction, see e.g., [26]. It is remarked that in these two approaches, additional devices on the hull structure have to be incorporated and additional energy input has to be made in the active one. In the present paper, without weight penalty (in the context of composite hulls) we investigate the efficiency of elastic tailoring on the alleviation of the whipping response. As discussed at the beginning, one basic variable enabling one to achieve elastic tailoring stems from the directionality property of composite materials.

Figures 4 and 5 compare the whipping responses of two cases: $[30_6]$ and $[90_6]$. It is remarkable to notice that significant reduction of the whipping intensity can be achieved by applying the tailoring technique. It is noted that the only difference within these two cases are on the ply angle. Using the results from Fig.6, it is concluded that such reduction is achieved by the dramatic increase of the stiffness coefficient a_{22}.

Another design variable for elastic tailoring is the lay-up. The corresponding design space is huge and many practical constraints have to be considered and optimization has to be used. Here, we compare only two cases: $[90/45/-45]_s$ and $[45_6]$. The results are shown in Figs.7 and 8. Again, notice the significant reduction of the whipping intensity by the lay-up $[90/45/-45]_s$.

8 Conclusions

In the context of slender marine vehicles made of advanced composite materials, a refined first-order transverse shearable anisotropic, moderately thick-walled beam theory is adopted to model the global dynamic behavior of the hulls. Exotic elastic couplings, transverse shear and warping are systematically incorporated. In the case of circumferentially asymmetric stiffness (CAS) lay-up with respect to the horizontal axis y, by integrating the unsteady hydrodynamic load, the comprehensive hydroelastic governing systems are derived. Exact modal solutions of some special cases are obtained. These analytical results can be used to calibrate the accuracy of numerical approaches and to facilitate the understanding of the role played by the material anisotropy and lay-ups on the change of dynamic behaviors of dry hulls.

It is further demonstrated by two simple cases, that the elastic tailoring can be effectively used to reduce the whipping intensity.

Acknowledgment

This work has been financially supported by the Office of Naval Research (Composites Program) under Grant No. N00014-06-0913. The financial support, the interest and encouragement of the Grant Monitor, Dr. Y. D. S. Rajapakse, are gratefully acknowledged.

References

[1] Bishop R. E. D., Price W. "*Hydroelasticity of Ships*". Cambridge University Press, Cambridge, Great Britain, 1979, p. 8.

[2] Xia J., Wang Z. and Jensen J. "Non-linear wave loads and ship responses by a time-domain strip theory". *Marine Structures,* Vol. 11, pp 101-123, 1998.

[3] Pedersen P. T. "Beam theories for torsional-bending response of ship hulls". *Journal of Ship Research,* Vol. 35, No. 3, pp 254-265, 1991.

[4] Wu J.-S., Ho C.-S. "Analysis of wave-induced horizontal-and-torsion-coupled vibrations of a ship hull". *Journal of Ship Research,* Vol. 31, No. 4, pp 235-252, 1987.

[5] Miao S., Price W. "Coupled bending and twisting vibrations of beam like structures". *Procedings of Dynamics of Marine Vehicles and Structures in Waves*, Price W.G., Temarel P. and Keane A. J. (editors), Elsevier Science Publishers, 1991.

[6] Bishop R. E. D., Cannon S. M., Miao S. "On coupled bending and torsional vibration of uniform beams". *Journal of Sound and Vibration,* Vol. 131, No. 3, pp 457-464, 1989.

[7] Bishop R. E. D., Price W. G., Zhang X. "A note on the dynamical behavior of uniform beams having open channel section". *Journal of Sound and Vibration*, Vol. 99, No. 2, pp 155-167, 1985.

[8] Shirk M. H., Hertz T. J., Weisshaar T. A. "Aeroelastic tailoring—theory, practice and promise". *Journal of Aircraft,* Vol. 23, No. 1, pp 6-18, 1986.

[9] Librescu L., Thangjitham S. "Analytical studies on static aeroelastic behavior of forward-swept composite wing structures". *Journal of Aircraft,* Vol. 28, No. 2, pp 151-157, 1991.

[10] Song O. "*Modeling and response analysis of thin-walled beam structures constructed of advanced composite materials*". Ph.D. thesis, Virginia Polytechnic Institute and State University, 1990.

[11] Librescu L., Meirovitch L., Song O. "Refined structural modeling for enhancing vibrations and aeroelastic characteristics of composite aircraft wings", *La Recherche Aérospatiale,* No. 1, pp 23-35, 1996.

[12] Qin Z., Librescu L. "Static and dynamic validations of a refined thin-walled composite beam model". *AIAA Journal*, Vol. 39, No. 12, pp 2422-2424, 2001.

[13] Hayman B. "Response of sandwich structures to slamming and impact loads". *Composite Materials in Marine Structures*, Vol. 2, Chapter 9, Edited by Shenoi R. A. and Wellicome J. F., Cambridge University Press, Cambridge, Great Britain, 1993.

[14] Faltinsen O. M. "Hydroelastic slamming". Journal of Marine Science and Technology, Vol. 5, pp 49-65, 2000.

[15] Librescu L., Song O. "*Thin-Walled Composite Beams: Theory and Application*". Solid Mechanics and Its Applications Series, Vol. 131, Springer, The Netherlands, pp 574-586, 2006.

[16] Rehfield L. W. "Design analysis methodology for composite rotor blades". *7th DoD/NASA Conference on Fibrous Composites in Structural Design*, Denver, CO, Jun 17-20.

[17] Librescu L., Song O. "Behavior of thin-walled beams made of advanced composite materials and incorporating non-classical effects". *Applied Mechanics Reviews*, Vol. 44, No. 11, part 2, pp S174-S180, 1991.

[18] Song O., Librescu, L. "Free vibration of anisotropic composite thin-walled beams of closed cross-section contour". *Journal of Sound and Vibration*, Vol. 167, No. 1, pp 129-147, 1993.

[19] Meirovitch L. "Principles and Techniques of Vibrations", Prentice Hall, Upper Saddle River, New Jersey, pp 82-86, 1997.

[20] Huang T. "The effect of rotary inertia and of shear deformation on the frequency and normal mode equations of uniform beams with simple end conditions". *Transactions of the ASME Journal of Applied Mechanics*, Vol. 28, pp 579-584, 1961.

[21] Belik O., Bishop R., Price W. "Influence of bottom and flare slamming on structural responses". *Trans. RINA*, Vol. 130, pp 261-275, 1988.

[22] Mizoguchi S., Tanizawa K. "Impact wave loads due to slamming-a review". *Ship Technology Research*, Vol. 43, pp 139-154, 1996.

[23] Bishop R., Price, W., Tam P. "On the dynamics of slamming". *Trans. RINA*, Vol. 120, pp 259-280, 1978.

[24] Stavovy A., Chuang S.-L. "Analytical determination of slamming pressures for high-speed vehicles in waves". *Journal of Ship Research*, Vol. 20, No. 4, pp 190-198, 1976.

[25] Belik O., Bishop R., Price W. "On the slamming response of ships to regular head waves". *Trans. RINA*, Vol. 122, pp 325-337, 1980.

[26] Hsueh W.-J., Lee Y.-J. "Reduction of hull whipping in slamming by active control system". *Journal of Ship Research*, Vol. 38, No. 2, pp 115-122, 1994.
[27] Jones N. "Slamming damage". *Journal of Ship Research*, Vol. 17, No. 2, pp 80-86, 1973.

Table 1. Material properties and geometric specifications of the idealized composite hull used in the investigation of slamming impact.

Material	**Value**
E_{11}	$1.42\times10^{11} N/m^2$
$E_{22}=E_{33}$	$9.79\times10^{9} N/m^2$
$G_{13}=G_{23}$	$6.0\times10^{9} N/m^2$
G_{12}	$4.83\times10^{9} N/m^2$
$(\mu_{12},\mu_{13},\mu_{23})$	$(0.24, 0.24, 0.5)$
ρ_s	$1.60\times10^{3} Kg/m^3$
Geometric	**Value**
Width[a]	$10m$
Depth[a]	$7m$
Wall thickness (h)	$0.5m$
Number of layers	6

[a] The length is measured on the mid-line contour

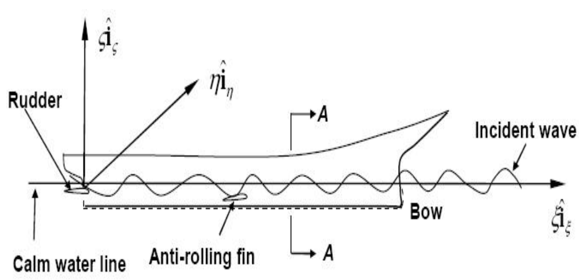

Fig.1. An advanced composite marine craft in wavy sea.

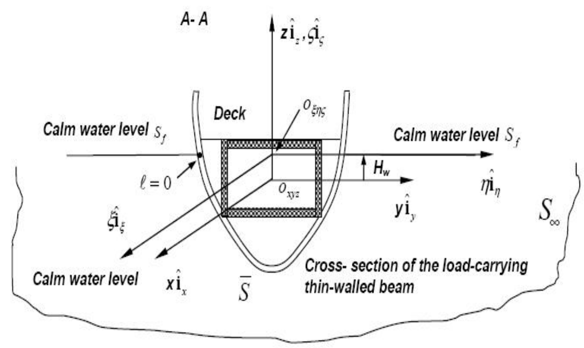

Fig.2. An idealized profile of the composite marine craft in Fig.1. The CAS lay-up configuration with respect to the axis y is used, i.e., the ply angle μ on the flanges (top and bottom walls) and the webs (right and left walls) fulfill $\theta(-y)=-\theta(y)$.

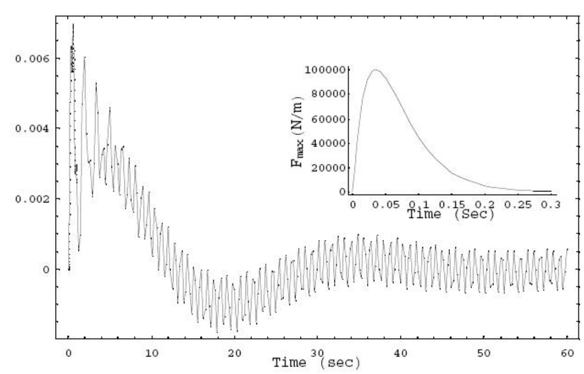

Fig.3. Hydroelastic response $u_{30}(x/L=0.5,t)$ amidship subject to a single slam impact.

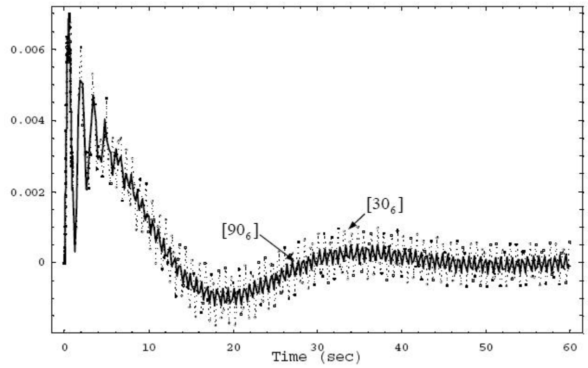

Fig.4. Influence of elastic tailoring on the hydroelastic response $u_{30}\,(\,x/L = 0.5, t\,)$ amidship subject to a slam impact.

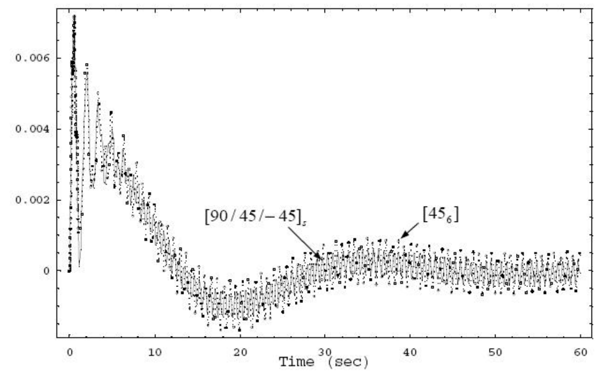

Fig.7. Influence of elastic tailoring on the hydroelastic response $u_{30}\,(\,x/L = 0.5, t\,)$ amidship subject to a slam impact.

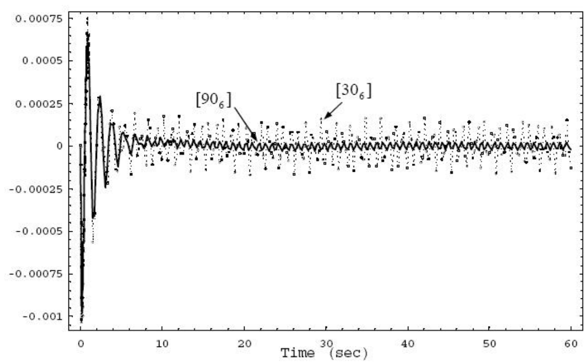

Fig.5. Influence of elastic tailoring on the hydroelastic response θ_y $(\,x/L = 0.5, t\,)$ amidship subject to a slam impact.

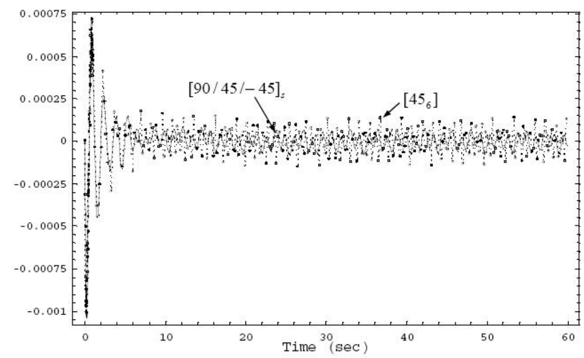

Fig.8. Influence of elastic tailoring on the hydroelastic response θ_y $(\,x/L = 0.5, t\,)$ amidship subject to a slam impact.

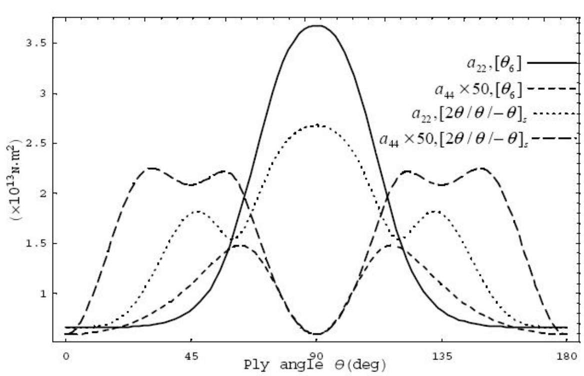

Fig.6. Cross-sectional stiffness versus the ply angle.